Theor Appl Climatol (2009) 96:179–189
DOI 10.1007/s00704-008-0022-8

ORIGINAL PAPER

A hydrological onset and withdrawal index for the West African monsoon

G. A. Dalu · M. Gaetani · M. Baldi

Received: 19 October 2006 / Accepted: 27 December 2007 / Published online: 24 April 2008

Abstract We have developed a hydrological prognostic index, *HOWI* (hydrological onset and withdrawal index), for the onset and the withdrawal of the West African monsoon (WAM), based on the vertically integrated moisture transport (*VIMT*). The regions of West Africa with the same climatological onset (withdrawal) date are characterized by a large change of the *VIMT* around the onset (withdrawal) date. By analyzing the variability of the *VIMT*, we determine the extension and the geographical position of these regions, which we take sufficiently large to filter out the fast weather variability. It turns out that the regions with the same climatological onset date do not usually coincide with the regions with the same climatological withdrawal date, the areas with the maximum variability of the *VIMT* during the onset phase are usually a fraction of the area where the variability of the *VIMT* is large during the withdrawal phase. This is because the onset has active phases and pauses in time and it is fragmented in space, while the withdrawal is rather rapid and almost uniformly distributed through the entire monsoonal region. When the monsoon moves inland, the rainfall slightly trails behind the arrival of the moisture, and, when the monsoon moves back towards the gulf of Guinea, the moisture slightly precedes the retreating rainfall. In a specific region, we say that the onset (withdrawal) of the monsoon occurs when the moisture reaches (declines to) half of its climatological value. The level of the moisture relatively to its climatological value is evaluated through the *HOWI*, i.e., at the onset (withdrawal) the *HOWI* is zero with a positive (negative) tendency. We find that the dates of the onset of the monsoon determined using the *HOWI*, computed in the region where the *VIMT* has its maximum variability during the onset phase of WAM, well agree with the dates of the sudden transition of the ITCZ (Intertropical Convergence Zone) from 5 to 10°N. The uncertainty on the onset date is of the order of 2 pentads, which is comparable to the uncertainty on the date of the sudden transition of the ITCZ. We, then, use the *HOWI* to determine the onset and the withdrawal dates of the monsoon for the period 1979–2004, finding that an early (late) onset usually preludes to a longer (shorter) monsoonal season with more (less) cumulated rain. Finally, we compare the onset dates in the Sahelian region, for the period 1979–2004, with those determined using methods based on rainfall.

G. A. Dalu · M. Gaetani · M. Baldi (✉)
Institute of Biometeorology,
Via Taurini,
19-00185 Rome, Italy
e-mail: m.baldi@ibimet.cnr.it

G. A. Dalu · M. Baldi
NIWA,
Auckland, New Zealand

1 Introduction

Monsoons are large-scale perturbations of the tropical atmospheric flow induced by the ocean-continent seasonal temperature contrast, which changes the wind direction driving the ocean moisture inland and causing abundant rainfall. Specifically, the West African monsoon (WAM) originates in the Gulf of Guinea when the thermal sea-land contrast turns the flow in the planetary boundary layer (PBL) to southwesterly, advecting ocean moisture inland and triggering the monsoonal rainfall. The West African monsoon activity spans from 5°N up to 20°N, with the amount of the rainfall cumulated during the monsoonal season monotonically decreasing with latitude northward of 8–10°N, and with the monsoonal rain and moisture barely reaching as far as the northern edge of this area (Fig. 1).

The WAM rainfall shows a long-term trend and an intraseasonal variability. An analysis of the rainfall in the second half of the past century shows a decadal trend where the years 1950–1970 were wetter than the years 1971–1990 (Poccard et al. 2000; Le Barbe' et al. 2002). A wavelet analysis of the rainfall shows a quasi-periodicity at 5, 15, and 45 days (Janicot and Sultan 2001), and from the intrinsic variability of the fast signals related to the synoptic weather features, we deduce that the inherent uncertainty on the onset date in a specific site is of the order of one-two pentads.

The importance of having a good index for the onset of WAM is due to the fact that the onset and the duration of the monsoon is critical for the Sudan-Sahel countries, since their economy is based mainly on farming. In fact, agricultural production is the most weather-dependent among human activities (Hansen 2002), and the knowledge of the date of the onset of the rainy season as well as its duration and total amount of rainfall are crucial factors on which decision-makers and farmers have to rely for crops and water management for suitable contingency plans (Sultan et al. 2005).

Empirical methods based on rainfall amounts have been developed in order to estimate the onset date of the monsoon. For instance, Ilesanmi (1972) identify the onset and the retreat of the monsoon in Nigeria using prescribed percentiles of the cumulated rainfall. Since the monsoon establishes itself through active phases and pauses (Janicot and Sultan 2001), taking advantage of this fact, Sultan and Janicot (2003) distinguish the preonset from the onset phase: the preonset occurs in late spring when the intertropical convergence zone (ITCZ) reaches 5°N, while the actual onset of the monsoon occurs in late June when the ITCZ shifts suddenly northward reaching 10°N. This transition of the ITCZ usually occurs during the active phase after the third pause of the monsoon (Louvet et al. 2003).

Other methods are based on surface variables other than the rainfall. Li and Zeng (2002) use the 925-hPa wind seasonal variation for their unified monsoonal index. Omotosho et al. (2000) use the equivalent potential temperature to predict the onset and the cessation of the rainy season in Kano (12°N, 8°E, Nigeria). Analyzing the period 1962–1996, Odekunle et al. (2005) find the onset and retreat dates in Nigeria using a stepwise multiple linear regression analysis. Their analysis is based on four promoting factors or predictors: the sea surface temperature in the tropical Atlantic, the land-sea thermal contrast between the Atlantic and Nigeria, the position of the intertropical discontinuity (ITD), and the surface temperatures in selected Nigerian sites. The validity of the last two methods is based on the fact that the dynamics of the monsoon is regulated by the meridional gradient of the boundary-layer entropy (Eltahir and Gong 1996), and, in more general terms, by the gradient of the moist static energy, *MSE* (Eq. 1), which accounts not only for the entropy, but also for the geopotential and the latent heat (Polcher 1995).

Therefore, aiming to the construction of an index for the onset and withdrawal of the monsoon, we consider *MSE* as a good candidate. However, wanting an index good in specific regions, we will show that the *MSE* is a weak indicator of the arrival of the monsoon. In fact, the gradients of its components have an opposite sign in the transition zone between two adjacent regions, one reached and the other not yet reached by the monsoon, since the latent heat is large and the entropy is small in the first one, while the vice versa is true in the second one. Through the analysis of the behavior of the *MSE* components, we will show that the moisture arrival in (retreat from) a specific region is the best indicator of the arrival (withdrawal) of the monsoon.

1.1 Data

We use the wind and the specific humidity data of the NCEP/DOE reanalysis (Kanamitsu et al. 2002), and the

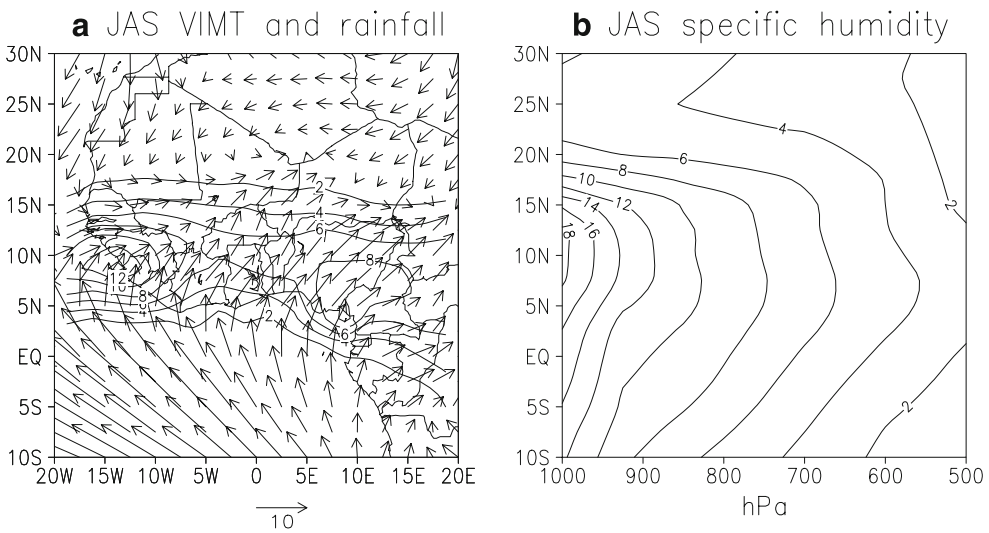

Fig. 1 **a** PBL vertical integrated moisture transport vector, **VIMT**, [hPa (m s^{-1})] and rainfall [mm day^{-1}], averaged through the monsoonal season (JAS). **b** Vertical cross section of the specific humidity averaged through JAS and zonally averaged between 10°W and 10°E [gr kg^{-1}]

rainfall pentad data of the Global Precipitation Climatology Project, GPCP (Xie and Arkin 1997; Xie et al. 2003), a merge of gauge and satellite observations. The dataset has a resolution of 2.5×2.5°, with a half mesh (1.25°) of spatial offset between the rainfall and the reanalysis variables. Pentad rainfall data have been run through a three-point filter. Daily NCEP/DOE data have been averaged in pentads and run through a three-point filter.

The *VIMT* behavior is analyzed in the work region 10°W–10°E and 5°–20°N (Fig. 5c), hereafter identified as the Wider Domain (WD), and in subregions of the WD, through the years 1979–2004. Within this period the dataset is relatively homogeneous (Trenberth et al. 2001), and, in addition, the onset determined using *HOWI* can be checked with the onset given for these years by Sultan and Janicot (2003) and by Louvet et al. (2003), in order to verify the validity of the method.

2 The hydrological onset and withdrawal index, *HOWI*

2.1 The search of the relevant parameters

In the search of the relevant parameters on which to base such an index, robust also where the monsoon rainfall is usually scarce, we analyze the behavior of several param-

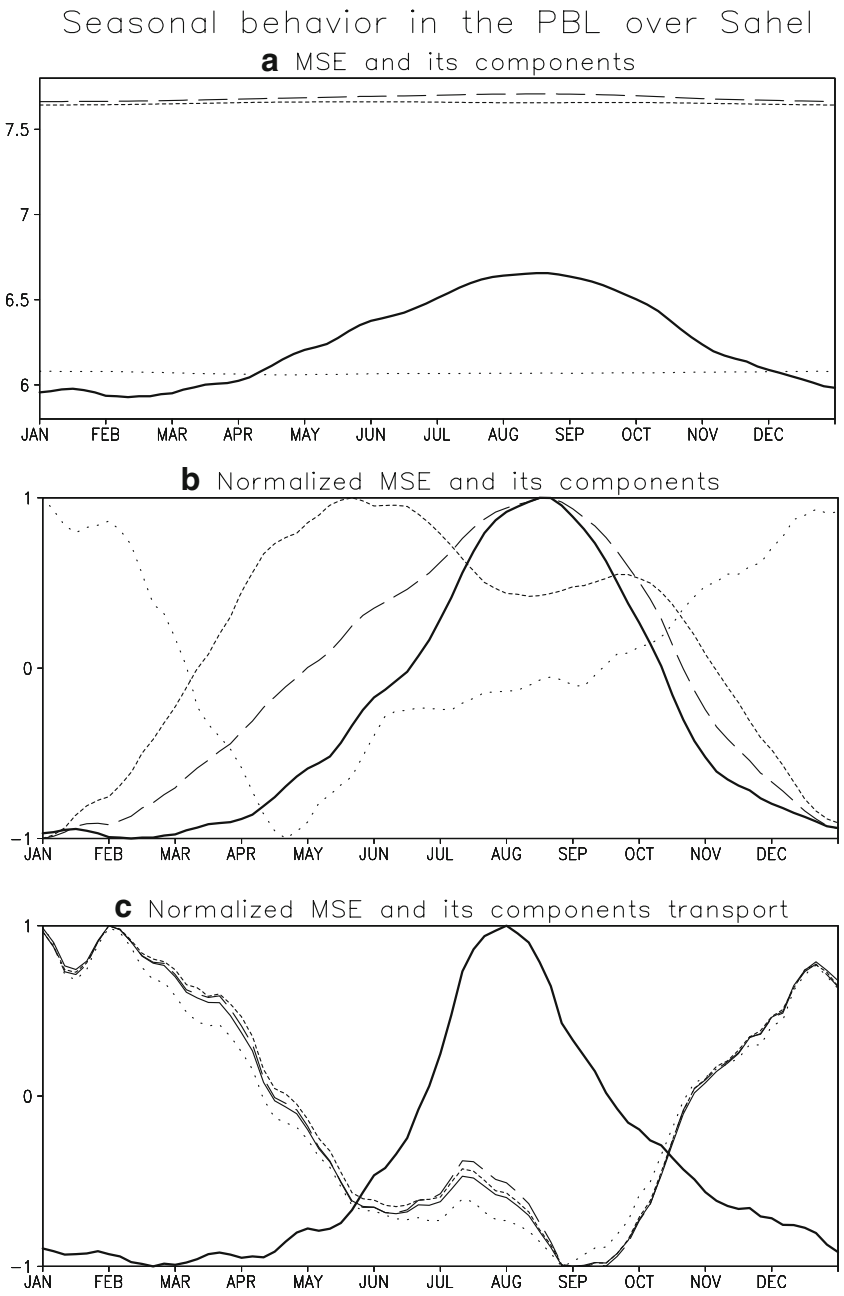

Fig. 2 *MSE* and components, vertically integrated in the PBL: wind, *solid line*; *MSE*, *dashed line*; entropy, *short dashed line*; geopotential *dot*; latent heat, *thick solid line*. **a** $\log_{10}(\overline{MSE})$, $\log_{10}(\overline{C_pT})$, $\log_{10}(\overline{gz})$, and $\log_{10}(\overline{Lq})$. **b** Normalized *MSE* and components. **c** Normalized wind intensity, transport of the *MSE* and of its components: V_{norm}, $(V{\cdot}MSE)_{\text{norm}}$, $(V{\cdot}C_pT)_{\text{norm}}$, $(V{\cdot}gz)_{\text{norm}}$, and $(V{\cdot}Lq)_{\text{norm}}$

eters related to the wind and to the *MSE* in the Sahelian region (10°W–10°E, 13°N–18°N in Fig. 4c).

$$MSE = gz + C_pT + Lq \tag{1}$$

the first term is the geopotential, the second term is the entropy, and the last term is the latent heat. Following Fontaine and Philippon (2000), we find that a strong *MSE* gradient separates the monsoonal air from the desert air, and analyzing the behavior of each term, we find that $\partial_y MSE$ in the PBL is almost entirely made of $\partial_y(Lq)$, while the contribution of $[\partial_y(gz) + \partial_y(C_pT)]$ is almost negligible. Then we analyze the behavior of the *MSE* and of its components in the PBL in the Sahel,

$$\overline{MSE} = \int_{p_{surface}}^{850hPa} MSE\ dp \text{ and } MSE_{norm} = 2\left\{\frac{\langle\overline{MSE}\rangle_A - \min\langle\overline{MSE}\rangle_A}{\max\langle\overline{MSE}\rangle_A - \min\langle\overline{MSE}\rangle_A}\right\} - 1 \tag{2}$$

where $\max\langle\overline{MSE}\rangle_A$ and $\min\langle\overline{MSE}\rangle_A$ are the maximum and the minimum of the climatological *MSE* vertically integrated in the PBL (overline), and horizontally averaged over the region $A \equiv$ Sahel. The behavior of $\overline{MSE}$ and of its components is shown in Fig. 2a: the latent heat peaks in the monsoonal season, while the geopotential and the entropy are almost flat, the entropy is by far the largest term (the y-axis is logarithmic, $\log_{10}$), this fact weakens the peak of the *MSE* in the monsoonal season. In order to focus on the different behaviors, we normalize *MSE* and its components as in Eq. (2). The results are shown in Fig. 2b: $(C_pT)_{\text{norm}}$ has a maximum before the monsoonal season (MJ) and a relative maximum in fall (SO), $(gz)_{\text{norm}}$ peaks in winter (DJF) in opposition with the monsoonal season, while the $(MSE)_{\text{norm}}$ and $(Lq)_{\text{norm}}$ peak right in the middle of the monsoonal season (AS), confirming that *MSE* and Lq are the good indicators. Since C_pT and gz peak off the monsoonal season, the peak of the *MSE* in the monsoonal season is entirely due to Lq. Progressing in our analysis, we study the behavior of the wind in the PBL,

$$\overline{V} = \int_{p_{surface}}^{850hPa} \sqrt{u^2+v^2}\ dp \text{ and } V_{norm} = 2\left\{\frac{\langle\overline{V}\rangle_A - \min\langle\overline{V}\rangle_A}{\max\langle\overline{V}\rangle_A - \min\langle\overline{V}\rangle_A}\right\} - 1 \tag{3}$$

we find that V_{norm} is strong in DJFM and weak in JJAS, with a relative small secondary maximum during the monsoonal season (Fig. 2c), and this makes an index based only on wind relatively weak. Analyzing the horizontal transport $(MSE{\cdot}V)_{\text{norm}}$ and the transport of each of the *MSE* components, we find that $(MSE{\cdot}V)_{\text{norm}}$, $(C_pT{\cdot}V)_{\text{norm}}$, and $(gz{\cdot}V)_{\text{norm}}$, since they are almost flat (Fig. 2a), behave very much like the wind (Fig. 2c), while the vertically integrated latent heat transport, $VIMT \equiv (Lq{\cdot}V)_{\text{norm}}$ in Eq. (4), has a very well defined single maximum in the monsoonal season, with an almost negligible amplitude outside this season (Fig. 2c). The product $(Lq{\cdot}V)_{\text{norm}}$ has the nice property of removing the winter maximum of the wind and of transforming the small summer relative maximum of the wind into a single well-peaked maximum. From the above results, we conclude that the moisture transport vertically integrated in the PBL is a good candidate for the construction of an index for WAM.

We have restricted the horizontal moisture transport to the PBL, since this is where the *VIMT* is stronger, because the moisture in WAM is mainly confined in the lower troposphere (Fig. 1b). Therefore, in developing the *HOWI* for WAM, we do not integrate it through the depth of the entire troposphere as Fasullo and Webster (2003) did for the Indian monsoon. In more general terms, we have introduced all the necessary modifications imposed by the different dynamics of the West African monsoon.

2.2 Behavior of the vertical integral of the moisture transport in the West African domain

The vertical integral of the moisture transport between the surface and the 850-hPa level is

$$\mathbf{VIMT} = \int_{p_{surface}}^{850hPa} (q \cdot \vec{v})\ dp \tag{4}$$

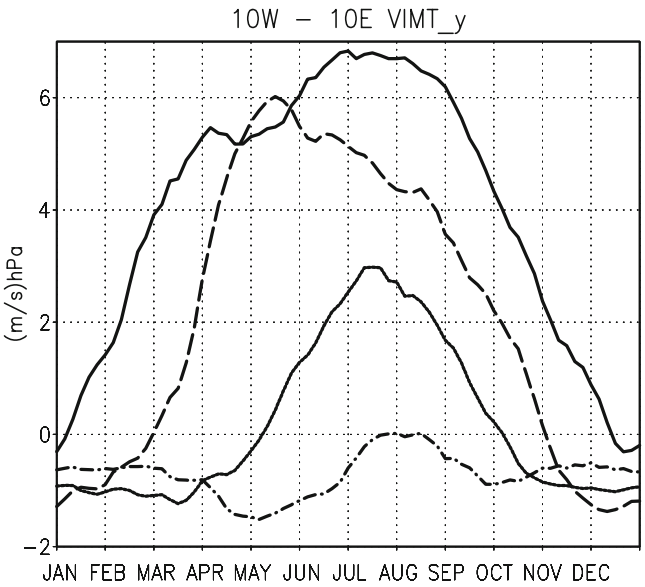

Fig. 3 Climatological behavior of the meridional component of the moisture transport, $\widehat{VIMT}_y$ [hPa (m s^{-1})], zonally averaged between x_1 = 10°W and x_2 = 10°E. $\widehat{VIMT}_y$ at 5°N (*solid line*), at 10°N (*dashed line*), at 15°N (*short dashed line*), at 20°N (*dash-dot line*)

$$\mathbf{VIMT} \equiv \left(VIMT_x, VIMT_y\right) \text{ and } VIMT = |\mathbf{VIMT}| = \sqrt{VIMT_x^2 + VIMT_y^2} \quad (5)$$

Through the monsoonal season, both components ($VIMT_x$, $VIMT_y$) contribute to the moisture transport; in addition, since most of the moisture comes from the Gulf of Guinea, the vertical integral of the moisture transport, **VIMT**, monotonically decreases with latitude, with small zonal variability (Fig. 1a). Analyzing the behavior of the climatological meridional moisture transport $\widehat{\overline{VIMT}_y}$ through four latitudes (5°N, 10°N, 15°N and 20°N in Fig. 3), and denoting the climatological value with an overbar and the zonal average with a hat,

$$\widehat{\overline{VIMT}_y} = \frac{1}{x_2 - x_1} \int_{x_1}^{x_2} \overline{qv}(x,y)\, dx \text{ with } x_1 = 10°\text{W and } x_2 = 10°\text{E} \quad (6)$$

we find that the meridional moisture transport, which is negative (southward) in winter, turns positive (northward) when the monsoon arrives at that latitude (Fig. 3), which is in agreement with the fact that the wind turns from northeasterly to southwesterly with the arrival of the monsoon (Sultan and Janicot 2003). Most of the moisture, which has gone through 5°N, reaches 10°N with a 7–8 pentads delay, this is also the lag between the preonset and the onset of the WAM defined by Sultan and Janicot (2003) as the jump of the ITCZ from 5°N to 10°N. Above 10°N the transport of the specific humidity monotonically decreases with latitude, with only half of the moisture reaching as far as 15°N.

None of the moisture from the Gulf of Guinea reaches as far as 20°N, this sets the northern most boundary of the WAM in the years 1979–2004 at this latitude. Actually, the flow of the moisture through the 20°N parallel is from the north for most of the year, and it is zero at the peak of the monsoonal season (Figs. 1a and 3), in fact, this moisture, which comes from the Mediterranean Sea, is very important for West Africa, and vital in the northernmost regions of WAM (Rowell 2003; Raicich et al. 2003).

Recalling that the moisture transport turns from northeasterly to southwesterly when a region is reached by the monsoon (Fig. 3), we examine the behavior of the vector

$$\Delta\overline{\mathbf{VIMT}}\,(x,y,t) = \overline{\mathbf{VIMT}}\,(x,y,t+10\ day) - \overline{\mathbf{VIMT}}\,(x,y,t-10\ day) \equiv \left(\Delta\overline{VIMT}_x,\ \Delta\overline{VIMT}_y\right) \quad (7)$$

It results that the northerly advancing monsoonal rain is pushed by the vigorous northward component of the $\Delta\overline{\mathbf{VIMT}}$ vector (Fig. 4a,b,c). When the monsoon retreats, the rain is pushed back southward by the negative meridional component of this vector (Fig. 5a,b,c). Around a given pentad (Eq. 7), the regions where $\Delta\overline{\mathbf{VIMT}}$ is large

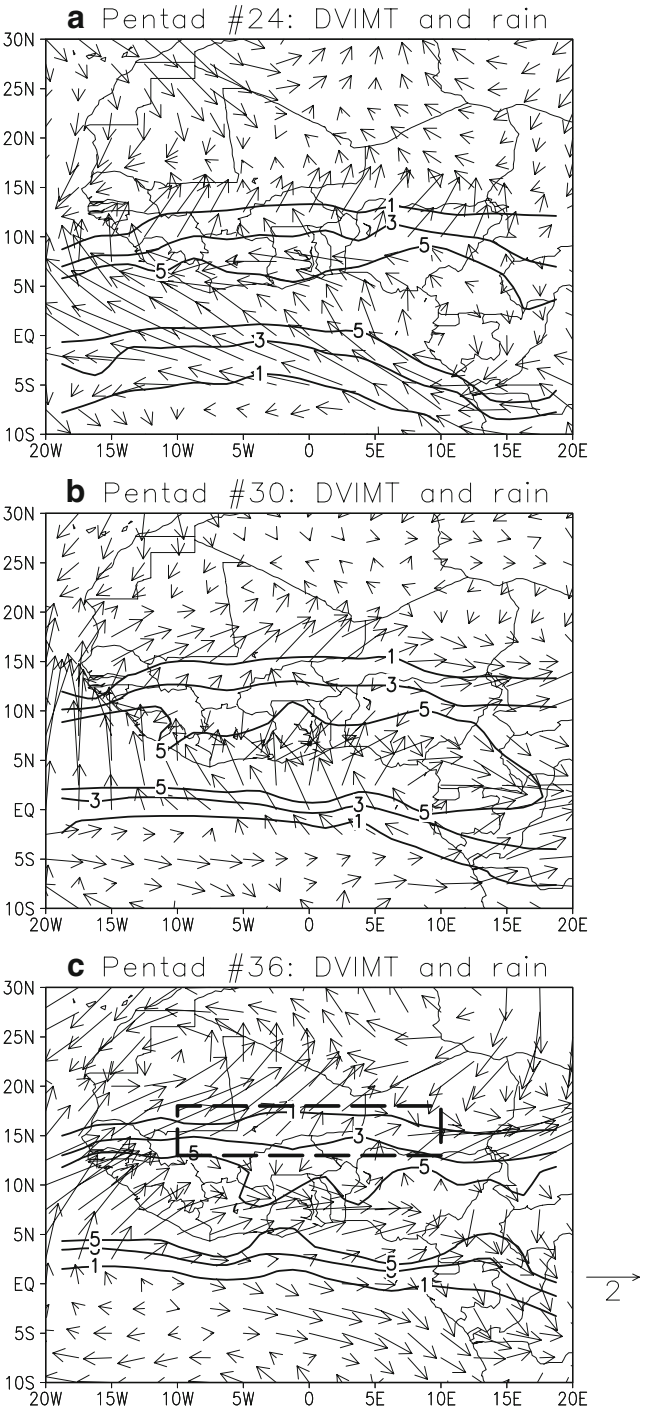

Fig. 4 Variability of the $\Delta\overline{\mathbf{VIMT}}$ vector [hPa (m s^{-1})] and of the rain belt [mm day^{-1}] as the monsoon moves northwards; **a** at t=24th pentad. **b** at t=30th pentad. **c** at t=36th pentad. The frame encloses the Sahel region (*dashed box*)

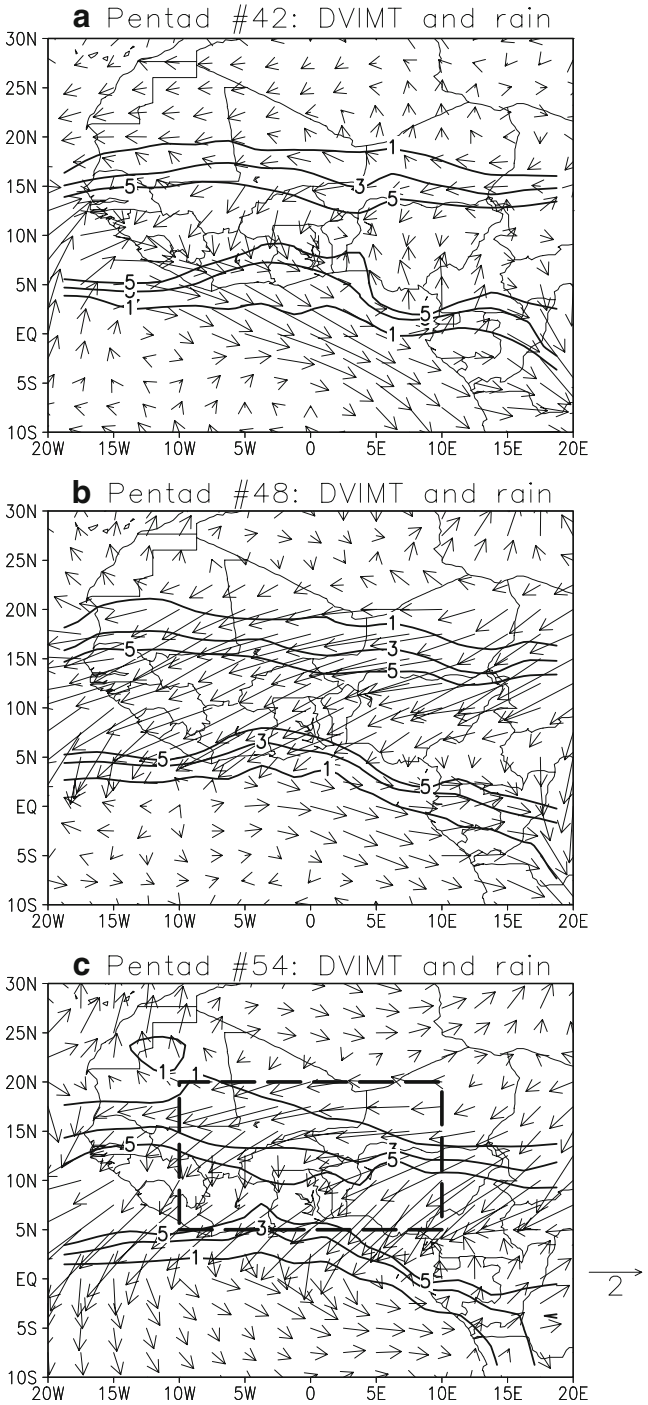

Fig. 5 Variability of the $\Delta\overline{\mathbf{VIMT}}$ and of the rain belt [mm day^{-1}] as the monsoon retreats southwards; **a** at t=42nd pentad. **b** at t=48th pentad. **c** at t=54th pentad. The frame encloses the WD (*dashed box*)

with about the same intensity $\left(\left|\Delta\overline{\mathbf{VIMT}}\right| \approx const\right)$ have the climatological onset (withdrawal), Fig. 4a,b,c and Fig. 5a,b,c. The regions with the same onset date are relatively small and fragmented (Fig. 4a,b,c), while the regions with the same withdrawal date are large and relatively uniform (Fig. 5a,b,c). Calling A one of these regions, we can compute the following integral

$$\langle \Delta\mathbf{VIMT}(t)\rangle_A = \frac{1}{A}\int_A \left[\Delta\mathbf{VIMT}(x,y,t)\right] dx\,dy \tag{8}$$

We could say that the onset (withdrawal) of the monsoon occurs in A when $<|\Delta\mathbf{VIMT}|(t)>_A$ reaches its maximum. However, since the time of this occurrence can be determined with some confidence only after the monsoon has established itself in A, this procedure has a limited practical value, therefore further elaboration is needed.

2.3 The hydrological onset and withdrawal index

Taking A large enough to filter out the weather disturbances, but sufficiently small so that the vector $\Delta\mathbf{VIMT}$ in the integrand in Eq. (8) is almost constant throughout A, we compute the average intensity of the vertical integral of the moisture transport (Eq. 4),

$$\langle VIMT\ (t)\rangle_A = \frac{1}{A}\int_A \left[VIMT(x,y,t)\right] dx\,dy \tag{9}$$

Since the desert air is very dry, while the monsoonal air is very moist, $<VIMT(t)>_A$ is very small before the arrival of the monsoon, it increases when the monsoon reaches A, to reach its maximum when A is completely filled with the moist monsoonal air. We use these nice properties to construct the *HOWI* as follows:

$$HOWI_A = 2\left\{\frac{\langle VIMT(t)\rangle_A - \min\langle\overline{VIMT}(t)\rangle_A}{\max\langle\overline{VIMT}(t)\rangle_A - \min\langle\overline{VIMT}(t)\rangle_A}\right\} - 1 \tag{10}$$

The onset occurs when the $HOWI_A$ becomes positive (the monsoonal air has filled half the region A), and the withdrawal occurs when it turns to negative values (half of the monsoonal air has left A). We like to emphasize that A has to be sufficiently large in order to make the index insensitive to the weather disturbances and robust to false (bogus) onsets and withdrawal, that A has to be sufficiently small since $\Delta\overline{\mathbf{VIMT}}$ has to be almost constant in A, and that the onset regions (Fig. 4a,b,c) may not in general coincide with the withdrawal regions (Fig. 5a,b,c).

The *HOWI* can be used for determining the onset dates of the monsoon in years before 1979, however, a detailed analysis of the hydrological regime is needed for each period in order to determine the sites with the same climatological onset date. For instance, the years 1950–1970 were much wetter than the years 1971–1990 (Poccard et al. 2000; Le Barbe' et al. 2002), the regions with the same climatological onset dates may be different in these

Table 1 Onset pentad and STD computed using different methods: the *HOWI*, the ITCZ shift, the pauses and active phases (PA), and the percentile method in the Sudan-Sahel (SUDSAH) and in the Sahel (SAH)

	HOWI	ITCZ	PA	SUDSAH	SAH
1979	34	36	38	35	34
1980	33	36	36	37	36
1981	33	36		35	35
1982	35	33	35	34	32
1983	39	36	37	35	35
1984	41	37	36	34	33
1985	34	31		37	37
1986	37	36	36	37	37
1987	40	37	39	37	36
1988	36	37	34	37	38
1989	39	37		38	39
1990	35	35		36	36
1991	37	38	33	34	34
1992	38	35	34	36	36
1993	38	34	38	37	37
1994	37	34	36	38	38
1995	36	34	34	36	36
1996	37	34	37	35	34
1997	36	37	39	33	34
1998	36	37	37	37	37
1999	39	34	33	39	39
2000	37	36	33	37	37
2001	34	34	39	37	36
2002	33	34		37	37
2003	30	37		36	36
2004	37	34		35	35
MEAN	36.2	35.3	36.0	36.1	35.9
STD	2.5	1.6	2.1	1.5	1.7

two periods, because of the change of the hydrological regime.

The onset dates, computed using the *HOWI* in the Sahel region (Fig. 4c) in the period 1979–2004, are shown in Fig. 7a and Table 1. The withdrawal dates in the larger monsoonal region WD (Fig. 5c) are shown in Fig. 7b and Table 2.

2.4 Onset in the Sahel and withdrawal in the WD, used as a benchmark

As an application of the *HOWI*, we study the onset of the monsoon in the Sahelian region (10°W–10°E, 13°N–18°N), and the withdrawal of the monsoon in the wider region, WD, (10°W–10°E, 5°N–20°N). The Sahel is a subregion of the WD.

The vector $\langle \Delta\overline{\mathbf{VIMT}}(t = 36^{th}pentad)\rangle_{Sahel}$ at the onset in the Sahelian region is shown in Fig. 4c. The climatological behavior of the $HOWI_{Sahel}$ is shown by the solid curve in Fig. 6a. The climatological onset in the Sahel in the period 1979–2004 occurs in the 36th pentad of the year (Fig. 7a and Table 1), and the climatological withdrawal is within the 53rd pentad of the year (Fig. 7b and Table 2). The uncertainty on the onset (25–29 June) and the uncertainty on the withdrawal (18–22 September) is of 2 pentads (Tables 1 and 2).

The vector $\langle \Delta\overline{\mathbf{VIMT}}(t = 54^{th}pentad)\rangle_{WD}$ at the withdrawal from the WD is shown in Fig. 5c. In the WD this vector is large with the exception of a relative minimum known as the Togo gap (Gu and Adler 2004). The climatological behavior of the $HOWI_{WD}$ is shown by the dashed curve in Fig. 6a. The climatological withdrawal date of the monsoon in the WD is about the same with about the same uncertainty as the withdrawal date in the Sahelian region (Fig. 6a and Table 2). This is because the rate at which the withdrawal of the monsoon occurs is uniformly rapid through the entire WD, as observed at surface stations by Odekunle (2006).

The uncertainty on the onset date in the WD is larger (smaller positive slope of the dashed line in Fig. 6a) than the uncertainty on the onset date in the Sahel (larger

Table 2 Withdrawal pentad and STD computed using different methods: the *HOWI* in the Sahel and in the WD, and the percentile method in the Sudan-Sahel (SUDSAH) and in the Sahel (SAH)

	HOWI	WD	SUDSAH	SAH
1979	59	52	54	54
1980	57	51	52	50
1981	53	53	52	52
1982	50	51	53	52
1983	52	52	52	52
1984	52	52	55	55
1985	53	53	52	52
1986	54	53	54	54
1987	52	54	54	54
1988	56	56	52	52
1989	48	52	53	53
1990	50	50	52	52
1991	50	50	54	53
1992	52	53	52	52
1993	54	52	53	53
1994	57	54	55	55
1995	54	57	54	53
1996	53	54	53	53
1997	51	52	53	52
1998	56	55	53	53
1999	50	53	54	54
2000	54	54	53	53
2001	55	55	53	53
2002	59	58	54	55
2003	54	60	53	52
2004	52	56	52	51
MEAN	53.3	53.5	53.1	52.8
STD	2.8	2.4	1.0	1.2

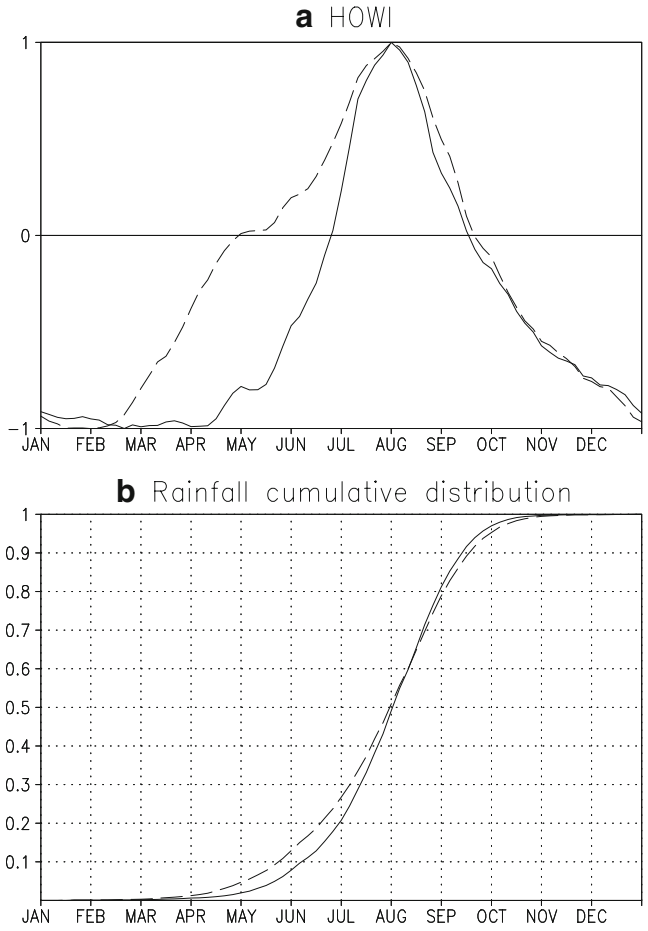

Fig. 6 **a** Climatological behavior of the *HOWI* computed in the Sahelian region (Fig. 4c), *solid line*, and in the WD (Fig. 5c), *dashed line*. **b** Climatological cumulated rainfall distribution in the Sahel (*solid line*) and in the Sudan-Sahel region (*dashed line*)

positive slope of the solid line in Fig. 6a). This is due to the fact that the different sub-regions of the WD have different onset dates, and that the onset date in the WD is the average of the onset dates of the different sub-regions composing the WD, the composite of their inherent uncertainties adds up to a larger uncertainty of the onset in WD.

3 Onsets and withdrawals determined using different methods

Since the knowledge of the onset, the duration, and the end of the precipitation period is very valuable, we assess the validity of the methodology by comparing the onsets and the withdrawals in the period 1979–2004 determined using the *HOWI* with those determined using other methods based on the rainfall.

For Sultan and Janicot (2003) the actual onset of WAM occurs with a steep decrease of the rainfall in the Guinean region followed by a steep increase in the Sudan-Sahel region, which is when the ITCZ transits from 5°N to 10°N. They give as a climatological date of the onset June 24, with a standard deviation of 8 days. For Louvet et al. (2003) the onset occurs with the active phase between the third and fourth pauses. Analyzing the period 1979–2001, they give as climatological onset the 36th pentad of the year (25–29 June), with a standard deviation of 2 pentads. For the period 1979–2004, the *HOWI* has an accuracy in determining the onset comparable to the accuracy of the methods developed by Sultan and Janicot (2003) and by Louvet et al. (2003), see Table 1 and in Fig. 7a. Sultan and Janicot method and Louvet et al. method have in common the use of the dynamical behavior of the rainfall for determining the onset of the monsoon. The *HOWI* is indirectly related to the previous two methods, since an accumulation of moisture above the threshold of one-half of the climatological value is needed to trigger the rain.

In addition, for the period 1979–2004, elaborating on the method developed by Ilesanmi (1972), who identifies the onset in Nigeria when the cumulated rainfall reaches 8% of the total, and the retreat when the cumulated rainfall reaches 90% of the total, we have evaluated that at the climatological *HOWI* onset the cumulated rainfall is 17% in the Sahel and 23% in the Sudan-Sahel region (10°W–10°E, 9°N–18°N), while, at the withdrawal, the cumulated rainfall is 93% in the Sahel and 91% in the Sudan-Sahel region (Fig. 6b). Based on this result, we have used the Ilesanmi method for diagnosing the onset and the withdrawal. For the withdrawal, the *HOWI* is tested using the percentile method (Table 2 and Fig. 7b). The percentile method shows standard deviations of the same order for the onset and lower for the withdrawal than the STD of the other methods (Tables 1 and 2). The uncertainty is minimized by the fact that the method is based on the actual cumulated rainfall, a datum available only when the entire monsoonal cycle has terminated. Therefore, being an a posteriori method, its main value is in its use as test of other methods. When compared, the different methods give about the same date for the onset with comparable STDs (Table 1), with the onsets within a band of ±2 pentads around the average value (Fig. 7a). Also the withdrawals (Table 2) fall within ±2 pentads around the average date of the withdrawal (Fig. 7b). The percentile method can be used to test other methods, and, the fact that its standard deviation is small, shows that these other methods can be further improved.

Using the *HOWI*, we estimate that the average duration of WAM is 17.2 pentads with a STD of 4.6 pentads, and that the average rainfall, cumulated between the onset and the withdrawal, is 451 mm with a STD of 107 mm. A further analysis shows that the duration of WAM is strongly anticorrelated to the date of the onset (r=-0.84 in Fig. 8a, a value exceeding the 99% level of significance), and that an

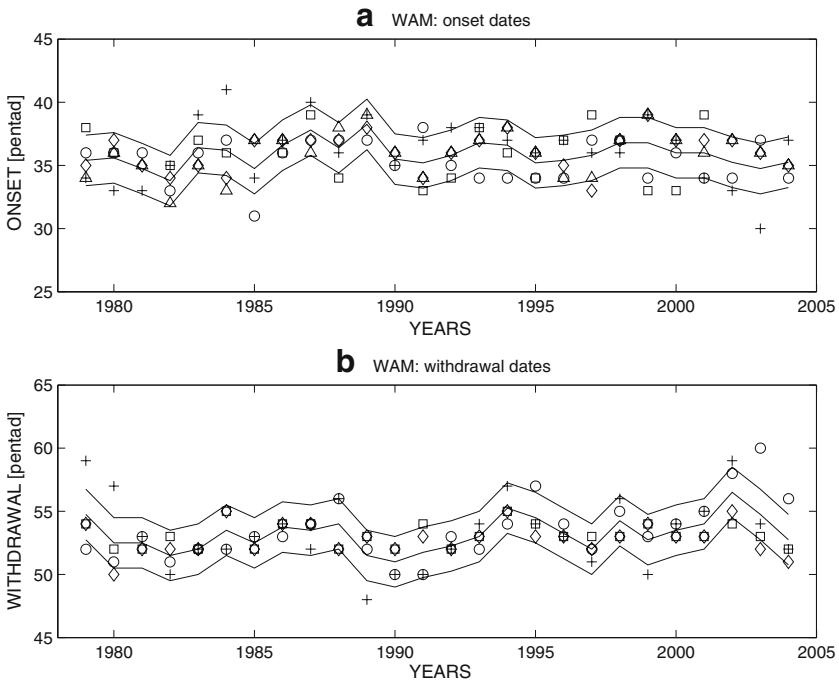

Fig. 7 **a** WAM onset evaluated using different methods: *HOWI* (*crosses*), ITCZ shift (*open circles*), pauses and active phases (*open squares*), percentile method in the Sudan-Sahel (*diamonds*), percentile method in the Sahel (*triangles*), and its average value (*central line within the ±2 pentad lines*); **b** WAM withdrawal evaluated using different methods: *HOWI* in the Sahel (*crosses*), *HOWI* in the WD (*open circles*), percentile method in the Sudan-Sahel (*open squares*), percentile method in the Sahel (*diamonds*), and its average value (*central line within the ±2 pentads lines*)

early (late) start usually preludes to a longer (shorter) monsoonal season, with more (less) cumulated rain (r=0.82 in Fig. 8b, a value exceeding the 99% level of significance). Specifically, in 2003 the *HOWI* gives an abnormally long monsoonal season (24 pentads, 1.5 STD above average), and large cumulated rainfall (672 mm, 2.1 STD above average), white bullets in Fig. 8. This is in agreement with the early onset reported by International Research Institute for Climate and Society (2003) and by Fontaine and Louvet (2006), and with the cumulated rainfall reported by Levinson and Waple (2004).

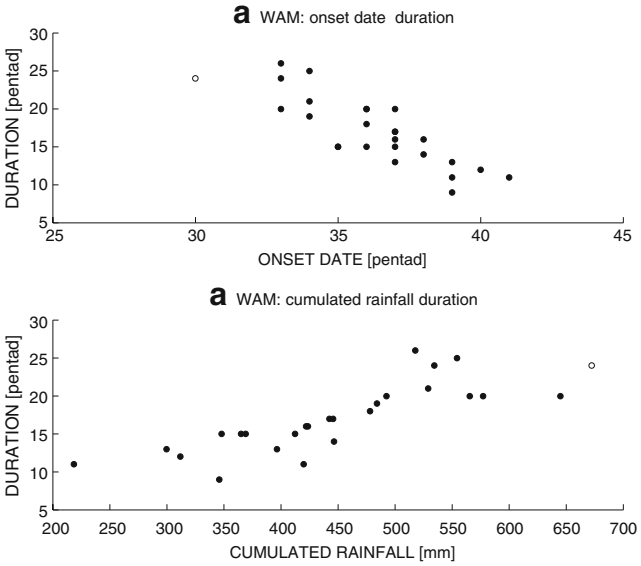

Fig. 8 **a** Bullets, correlation between the onset date and the duration of WAM in the Sahel, determined using the *HOWI*. *White bullet* refers to 2003. **b** Bullets, correlation between the seasonal cumulated rainfall and the duration of WAM in the Sahel, determined using the *HOWI*. *White bullet* refers to 2003

While the anticorrelation between the onset date and duration of the WAM is rather robust (Fig. 8a), the correlation between the duration and the cumulated rainfall is weak in years with well above or well below cumulated rainfall. The bullets are sparser in Fig. 8b than those in Fig. 8a. This behavior is due to the fact that uncertainty on the onset adds up to the uncertainty on the withdrawal in Fig. 8b, and that the uncertainties are larger in extreme cases. A longer record of good quality data is necessary to better quantify the above statements.

4 Conclusions

The rich phenomenology of WAM, with many space and time scales, makes a deterministic forecast of the onset and of the duration of the monsoon very difficult. Mohr (2004) finds that there is a daily pulsation of the convective activity, with, in addition, a synoptic scale pulsation (5–7 days) related to the easterly waves, which through baroclinic instabilities carries the rain to the Sudan-Sahel area (Diedhiou et al. 1999; Grist 2002; Grist et al. 2002). While the longer quasi-periodic modulation may be related to remote phenomena, such as a teleconnection with the Pacific warm pool through the Madden-Julian oscillation

(Knippers 2003; Matthews 2004). Semazzi and Sun (1997) relate the intraseasonal variability to the fluctuations (position and intensity) of the pressure high center over the Libyan desert. The many physical processes, with the different time scales involved, enhance the variability of the West African monsoon. Therefore the uncertainty of ±2 pentads on the onset, and of ±2–3 pentads on the withdrawal are probably inherent and intrinsic to this variability (Janicot and Sultan 2001). A ±2 pentads uncertainty corresponds to an 8% possible error on the evaluation of the cumulated rainfall at the onset, and a 5% possible error on the evaluation of the cumulated rainfall at the withdrawal.

Therefore, in order to filter out the fast weather variability, we select the areas where, in 2 pentads, the vertical integral moisture transport vector presents a large and homogeneous northwesterly (southeasterly) change. These regions have the same climatological onset (withdrawal) date. We say that the onset of the monsoon occurs in one of these regions when its area is half full of the monsoonal air ($HOWI \rightarrow 0_-$), or that the withdrawal occurs when half of the moist monsoonal air has left the region ($HOWI \rightarrow 0_+$). A reasonable estimate of the onset date of the monsoon with a 2–4 pentads lead time can be made monitoring the nearing of the *VIMT* to its climatological half value in the region, and monitoring the change of the sign of the *HOWI* to the south of the target region.

From the result shown in Table 1 and in Fig. 7a we conclude that in the period 1979–2004, the *HOWI* has an accuracy in determining the onset comparable to the accuracy of the methods developed by Sultan and Janicot (2003) and by Louvet et al. (2003). For the withdrawal, the *HOWI* can be tested only against the diagnostic percentile method (Table 2 and Figs. 6 and 7b). The *HOWI* can be used as a prognostic index for determining the onset of the monsoon in selected regions, with a performance comparable to the other prognostic methods. In addition, the *HOWI* gives a method for determining the withdrawal date. The uncertainty on these dates is slightly larger than that determined using the percentile method, showing that the *HOWI* can be further improved.

In addition, we find that the onset date and the duration of the rainy season are anticorrelated, and that the duration of the WAM and the cumulated rainfall are correlated. We have verified these results using the cumulated rainfall and the onset and withdrawal dates given by Omotosho et al. (2000) and Odekunle et al. (2005). This confirms that the *HOWI* is an effective index for the onset and the retreat of the WAM.

Specifically, in 2003 the monsoonal season was abnormally long with a large cumulated rainfall, this is when southwest Europe was affected by a long heat wave (Levinson and Waple 2004). This suggests a teleconnection between West Africa and the West Mediterranean regions, and further research is needed to substantiate this hypothesis.

Finally, since the percentile diagnostic method has a slightly smaller STD than the *HOWI*, it clearly indicates that a further improvement of 1/2 pentad on the onset and of 1 pentad on the withdrawal can be achieved in the future.

Acknowledgements NCEP Reanalysis data provided by the NOAA-CIRES ESRL/PSD Climate Diagnostics branch, Boulder, Colorado, USA (http://www.cdc.noaa.gov/). The GPCP combined precipitation data were developed and computed by the NASA/Goddard Space Flight Center's Laboratory for Atmospheres as a contribution to the GEWEX Global Precipitation Climatology Project. The onset pentads for the ITCZ shift method are computed using the daily onset dates available on the Benjamin Sultan's Web page at http://www.lodyc.jussieu.fr/~bslod/. Authors acknowledge the support of AMMA. Based on the French initiative, AMMA was built by an international scientific group and is currently funded by a large number of agencies, especially from France, the United Kingdom, the United States, and Africa. It has been the beneficiary of a major financial contribution from the European Community's Sixth Framework Research Programme. (Detailed information on scientific coordination and funding is available on the AMMA International Web site http://www.amma-international.org.). The paper benefits of the comments of the reviewers, the editor, and J. Salinger of NIWA. Authors are grateful to Mrs. Antonietta Falchi for professionally completing the editorial work. G. Dalu acknowledges the support of the Italian CNR *Short-Term Mobility Program*.

References

Diedhiou A, Janicot S, Viltard A, de Felice P (1999) Easterly wave regimes and associated convection over West Africa and tropical Atlantic: results from NCEP/NCAR and ECMWF reanalysis. Clim Dyn 15:795–822

Eltahir AB, Gong C (1996) Dynamics of wet and dry years in West Africa. J Climate 9:1030–1042

Fasullo J, Webster PJ (2003) A hydrological definition of Indian monsoon onset and withdrawal. J Climate 16:3200–3211

Fontaine B, Louvet S (2006) The Sudan-Sahel rainfall onset: definition of an objective index, types of years and experimental hindcasts. J Geophys Res 111:D20103, DOI 10.1029/2005JD007019

Fontaine B, Philippon N (2000) Seasonal evolution of the boundary layer heat content in the West African monsoon from the NCEP/NCAR Reanalysis (1968–1998). Int J Climatol 20:1777–1790

Grist JP (2002) Easterly waves over Africa, part I: the seasonal cycle and contrasts between wet and dry years. Mon Weat Rev 130:212–225

Grist JP, Nicholson SE, Barcilon AI (2002) Easterly waves over Africa, part II: observed and modeled contrasts between wet and dry years. Mon Weat Rev 130:212–225

Gu G, Adler RF (2004) Seasonal evolution and variability associated with the west African monsoon system. J Climate 17:3364–3377

Hansen JW (2002) Realizing the potential benefits of climate prediction to agriculture: issues, approaches, challenges. Agric Syst 74:309–330

Ilesanmi OO (1972) An empirical formulation of the onset, advance and retreat of rainfall in Nigeria. J Trop Geogr 34:17–34

International Research Institute for Climate and Society (2003) Climate Information Digest 6(7)

Janicot S, Sultan B (2001) Intraseasonal modulation of the convection in the West African monsoon. Geophys Res Lett 28:523–526

Kanamitsu M, Ebisuzaki W, Woollen J, Yang SK, Hnilo JJ, Fiorino M, Potter G (2002) NCEP-DOE AMIP-II reanalysis. Bull Am Met Soc 83:1631–1643

Knippers P (2003) Tropical-extratropical interactions causing precipitation in Northwest Africa: statistical analysis and seasonal variations. Mon Weat Rev 131:3069–3076

Le Barbe' L, Lebel T, Tapsoba D (2002) Rainfall variability in West Africa during the years 1950–90. J Climate 15:187–202

Levinson DH, Waple AM (2004) State of climate in 2003. Bull Am Met Soc 85 (6):S1–S72

Li J, Zeng Q (2002) A unified monsoon index. Geophys Res Lett 29 (8):2271, DOI 10.1029/2001GL013874

Louvet S, Fontaine B, Roucou P (2003) Active phases and pauses during the installation of the West Africa monsoon through 5-day CMAP rainfall data (1979–2001). Geophys Res Lett 30 (24):2271, DOI 10.1029/2003GL018058

Matthews AJ (2004) Intraseasonal variability over tropical Africa during northern summer. J Climate 17:2427–2440

Mohr KI (2004) Interannual, monthly, and regional variability in the wet diurnal cycle of precipitation in the Sub-Saharan Africa. J Climate 17:2441–2453

Odekunle TO (2006) Determining rainy season onset and retreat over Nigeria from precipitation amount and number of rainy days. Theor Appl Climatol 83:193–201

Odekunle TO, Balogun EE, Ogunkoya OO (2005) On the prediction of rainfall onset and retreat dates in Nigeria. Theor Appl Climatol 81:101–112

Omotosho JB, Balogun AA, Ogunjobi K (2000) Predicting monthly and seasonal rainfall, onset and cessation of the rainy season in the West Africa using only surface data. Int J Climatol 20:865–880 18

Poccard I, Janicot S, Camberlin P (2000) Comparison of rainfall structures between NCEP/NCAR reanalysis and observed data over tropical Africa. Clim Dyn 16:897–915

Polcher J (1995) Sensitivity of tropical convection to land surface processes. J Atmos Sci 52:3143–3161

Raicich F, Pinardi N, Navarra A (2003) Teleconnections between the Indian monsoon and Sahel rainfall and the Mediterranean. Int J Climatol 23:173–186

Rowell DP (2003) The impact of the Mediterranean SSTs on the Sahelian rainfall season. J Climate 16:849–862

Semazzi FHM, Sun L (1997) The role of orography in determining the Sahelian climate. Int J Climatol 17:581–596

Sultan B, Janicot S (2003) The West African Monsoon Dynamics. Part II: The "Preonset" and "Onset" of the Summer Monsoon. J Climate 16:3407–3427

Sultan B, Baron C, Dingkuhn M, Sarr B, Janicot S (2005) Agricultural impacts of large-scale variability of the West African Monsoon. Agric Forest Meteorol 128 (1–2):93–110

Trenberth KE, Stepaniak DP, Hurrell JW, Fiorino M (2001) Quality of the reanalysis in the tropics. Clim Dyn 14:1499–1510

Xie P, Arkin PA (1997) Global precipitation: a 17-year monthly analysis based on gauge observations, satellite estimates, and numerical model outputs. Bull Am Met Soc 78:2539–2558

Xie P, Janowiak JE, Arkin PA, Adler R, Gruber A, Ferraro R, Hu_man GJ, Curtis S (2003) GPCP pentad precipitation analyses: an experimental dataset based on gauge observations and satellite estimates. J Climate 16:2197–2214